Solid State Phenomena Vols. 192-193 (2013) pp 263-268

doi:10.4028/www.scientific.net/SSP.192-193.263

Squeeze Flow of Semi-Solid Slurries

Andreas N. Alexandrou[1], Georgios C. Florides[1] and Georgios C. Georgiou[2]

[1]Department of Mechanical and Manufacturing Engineering, University Cyprus
[2]Department of Mathematics and Statistics, University of Cyprus
P.O. Box 20537, 1678 Nicosia, Cyprus

Keywords: Squeeze flow; Bingham model; Thixotropy; Structural parameter; Computational rheology; Finite elements.

Abstract A standard method used to determine material properties of semi-solid slurries is the squeeze flow experiment in which a fixed amount of material is squeezed under constant force or velocity. The relation between the force and the displacement provides information about the rheology of the slurry. The thixotropy and the time response of the sample however is rarely, if ever, taken into consideration. In this work we study how thixotropy affects the flow characteristics and consequently the predicted material properties. We show that depending on the method of compression and the thixotropic constants the flow can be significantly different. Therefore the predicted material constants can vary and hence cannot be unique.

Introduction

The motivation of the present work of course comes from our interest in the processing of semi-solid metal (SSM) slurries. As it is well known, these relatively dense suspensions behave as viscoplastic fluids [1,2]. The viscoplastic behaviour is due to particle welding, dry friction, and hydrodynamic forces within the suspension. Semi-solid slurries also exhibit thixotropy, i.e. the viscosity decreases with time under constant shearing. The rheological properties of semi-solid slurries are partially reversible and partially irreversible [3]. The irreversible part is due to the breakage of the welded bonds between the particles. Given space limitations, we cannot review here and thus we simply refer the reader to the relevant literature, such as Favier and Atkinson [4], Modigell and Koke [5], Alexandrou and Georgiou [6], Gautham and Kapur [7], Koeune and Ponthot [8],

The objectives of the present work are: (a) to investigate numerically the squeeze flow experiment by accounting for thixotropy, and (b) to evaluate the use of the experiment to extract material constants in semisolid slurries. The consideration of thixotropy in rheometric flows has been also emphasized in [9,10,11,12].

Theoretical Model

As described in the introduction the finite yield stress τ_0 of SSM slurries is due to particle welding, dry friction, and hydrodynamic forces within the suspension. Here we assume that this viscoplastic behaviour can be described using the Bingham constitutive model [13,14]: $\underline{\underline{\dot{\gamma}}} = \underline{\underline{0}}$ for $\tau \le \tau_0$ and $\underline{\underline{\tau}} = \left(\tau_0 / \dot{\gamma} + \mu\right)\underline{\underline{\dot{\gamma}}}$ for $\tau > \tau_0$, where μ is the plastic viscosity, and $\underline{\underline{\tau}}$ and $\underline{\underline{\dot{\gamma}}}$ are the stress and rate-of-strain tensors, respectively.

Thixotropy is described using the traditional approach of the structural parameter, λ, which describes the state of the structure. When $\lambda = 1$ the material is fully structured and when $\lambda = 0$ the structure is fully broken [5,6,15]. The material parameters, i.e. the plastic viscosity and the yield stress are, in general, functions of λ [15].

In the present work, it is assumed that the plastic viscosity is constant. This is consistent with the experimental data of Modigell and Koke [5] where one observes a vertical shift of the flow curve with rest time (i.e. increase structure) and hence no significant change in the material constants. The vertical shift is due to the increase of the yield stress which increases with increasing structure [5]. Therefore during deformation as the structure breaks, the yield stress reduces. This dependence is expressed here using a simple linear relationship $\tau_y(t) = \lambda\tau_0$ where $\tau_y(t)$ is now the instantaneous yield stress.

For closure, the evolution of the structural parameter is assumed to follow the first-order rate evolution equation:

$$D\lambda/Dt=\alpha(1-\lambda)-b\lambda\dot{\gamma}e^{c\dot{\gamma}}$$

where $D\lambda/Dt$ is the material derivative, a is the recovery parameter, and b and c are the breakdown parameters determined from experimental data. The two terms in the RHS of the evolution equation describe the rates of structure build-up and break-down. The exponential in the second term accounts for the fact that the shear stress evolution in shear rate step-up experiments is typically faster than in the step-down ones.

In order to overcome the inherent singularity of the discontinuous Bingham constitutive relation we adopt the regularization proposed by Papanastasiou [16]:

$$\underline{\underline{\tau}} = \left\{\tau_o\lambda\left[1-\exp\left(-m\dot{\gamma}\right)\right]/\dot{\gamma}+\mu\right\}\underline{\underline{\dot{\gamma}}}$$

where m is the stress growth parameter. The equation is valid uniformly at all levels of $\dot{\gamma}$ and provides a satisfactory approximation of the Bingham plastic model for sufficiently large values of m [14,17].

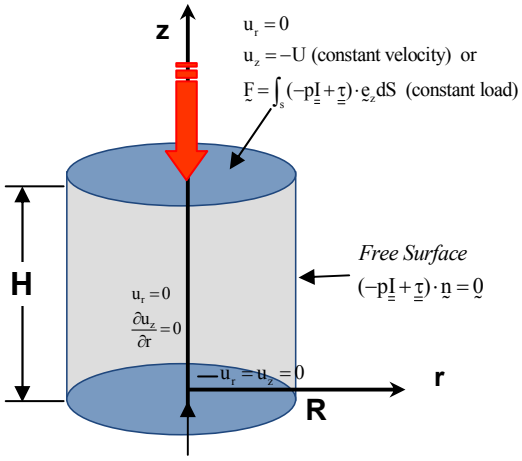

Figure 1: Geometry and boundary conditions of the squeeze flow experiment. At t=0 the sample is at rest.

Governing Equations

In squeeze flow, the material is placed between two parallel discs (Figure 1) and is compressed under constant load or constant velocity, while the lower disc remains fixed. The cylindrical sample is characterized by an initial radius R_0 and height H_0=2R_0. The continuity and momentum equations are:

$$\nabla\cdot\underline{u} = 0, \qquad \mathrm{Re}\frac{D\underline{u}}{Dt} = -\nabla p + \nabla\cdot\underline{\underline{\tau}}, \qquad \underline{\underline{\tau}} = \left[Bn\lambda\frac{1-\exp(-M\dot{\gamma})}{\dot{\gamma}}+1\right]\underline{\underline{\dot{\gamma}}}$$

where the Bingham, the growth number, the Reynolds and the non-dimensional force are defined by

$$\mathrm{Bn} = \frac{\tau_0 \mathrm{H}_0}{\mu \mathrm{U}}, \qquad \mathrm{M} = \frac{\mathrm{mU}}{\mathrm{H}_0}, \qquad \mathrm{Re} = \frac{\mathrm{rUH}_0}{\mathrm{m}}, \qquad \mathrm{F} = \frac{\overline{\mathrm{F}}}{\tau_0 \mathrm{H}_0^2}$$

In the case of squeeze flow under constant load, U is either an arbitrary velocity or it can be defined by $\mathrm{U} = \mathrm{F}/\mu \mathrm{H}_0$

The boundary conditions of the flow are also shown in Figure 1. Symmetry boundary conditions are imposed along the axis of symmetry and the velocity is set to zero along the bottom. On the free surface it is assumed that surface tension is zero. When the sample is compressed at constant load in the direction of gravity, i.e. the dimensionless load is of the form $\boldsymbol{F} = -F\,\boldsymbol{e}_z$, the boundary condition at the top of the sample is given by

$$\mathbf{F} = \int_S (-\mathrm{p}\underline{\underline{I}} + \underline{\underline{\tau}}) \cdot \mathbf{e}_z \, \mathrm{dS}$$

where S is the surface of the top, and $\underline{\underline{I}}$ is the unit tensor.

Numerical method

The flow problem is solved in Lagrangian coordinates. The governing equations are discretized using the mixed-Galerkin finite element method. The non-linear system of equations is solved using a Newton-Raphson iteration procedure with an error tolerance equal to 10^{-5}. Remeshing is achieved by using a Laplace-type discretization algorithm. Care is taken to construct a finer mesh at critical corners. More details can be found in [14].

Results and Discussion

The sample is compressed from rest either under constant load or constant. Three different meshes have been used, the characteristics of which are tabulated in Table 1. The numerical results are obtained using Mesh 2 (20×20), which gives converged results similar to those from the more refined Mesh 3. Similarly the value M=300 was found to be sufficiently high so that the regularized model provides a good approximation for the ideal Bingham model; no significant differences were observed from results obtained with M=800. The time step is fixed after extensive numerical experimentation and is kept constant throughout the simulation.

Table 1: Characteristics of the meshes used in the simulations

	Elements	Nodes	Unknowns
Mesh 1 (15X15)	225	961	2148
Mesh 2 (20X20)	400	1681	3763
Mesh 3 (24X24)	576	2401	5379

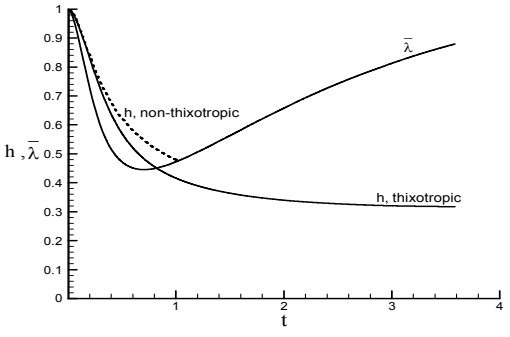

Figure 2: Height and structural parameter as a function of time (F=-1, Re=1, Bn=1,a=1, b=1, c=0.01).

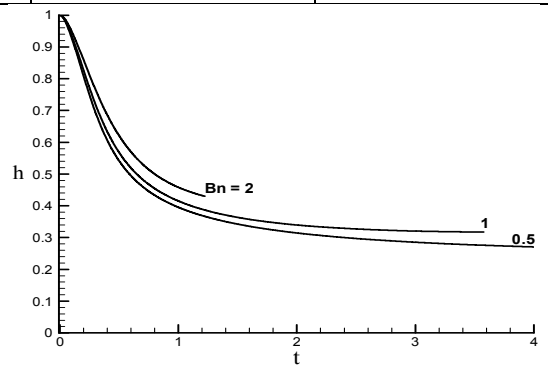

Figure 3: Height and a function to time for different Bn numbers (F=-1,Re=1,a=1,b=1,c=0.01)

Results are obtained for the evolution of the internal structure, the yielded and unyielded surfaces as well as all flow parameters. However, due to lack of space we will discuss only the evolution of the height and the mean structural parameter for few selected cases. Figure 2 shows that the height decreases monotonically and eventually reaches a plateau, which is, of course expected. For comparison purposes the height of a non-thixotropic sample (a=b=c=0) is also plotted. With the inclusion of the structural parameter the duration of the squeeze flow experiment increases. This is due to the fact that the structure breaks down, resulting in reduced yield stress. The mean structural parameter $\bar{\lambda}$ initially decreases reaching a minimum before the leveling of the sample height, after which build-up is observed.

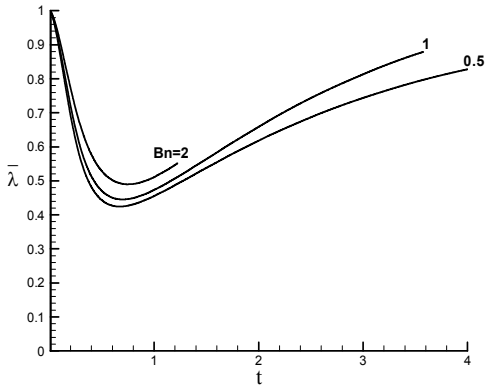

Figure 4: The average structure as a function of Bn (F=-1, Re=1, b=1, and c=0.01).

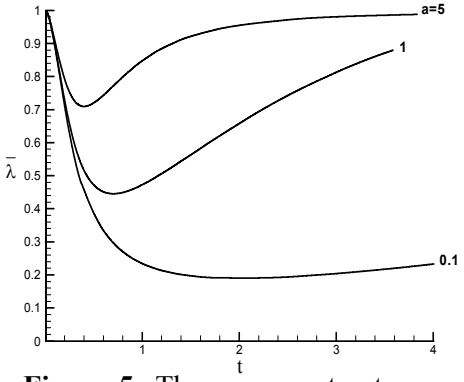

Figure 5: The average structure as a function of the buildup parameter (F=-1, Bn=1, Re=1, b=1, c=0.01)

The effect of the Bingham number on the height and the mean structural parameter is illustrated in Figures 3 and 4. In agreement with previous works for non-thixotropic yield stress fluids, the squeeze rate becomes lower and the final sample height increases with the Bingham number [11,14]. We observe that the break-down of the welded particles becomes slower at higher Bingham numbers and continues reaching a minimum value after which a build-up occurs. The resulting minimum is thus higher and is shifted to the right. In the build-up stage the material regains its structure faster as Bn increases, due to reduced shearing.

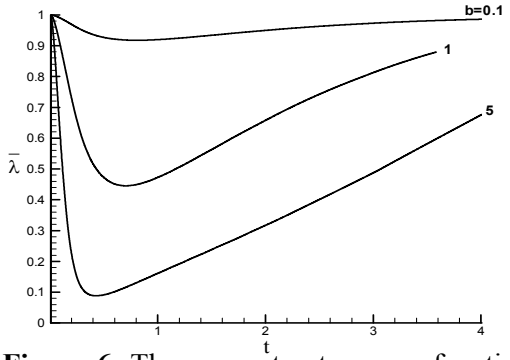

Figure 6: The mean structure as a function of the breakdown parameter (F=-1, Re=1, Bn=1, a=0.1, c=0.01)

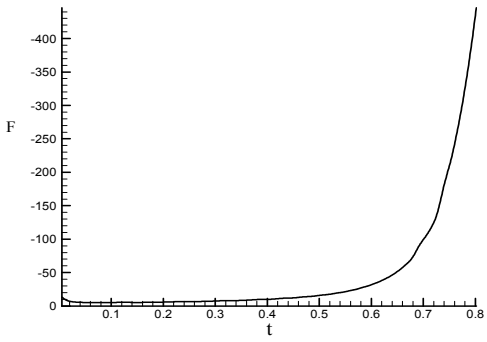

Figure 7: The load during compression at constant velocity (V=-1, Re=1, Bn=1, a=b=1, c=0.01)

The effects of the recovery and break-down parameters on the squeeze rate and the mean structural parameter of the base flow are illustrated in Figures 5 and 6, respectively. The squeeze rate appears not to be affected initially by a, but as the experiment proceeds, the flow decelerates at higher values of a with significant reduction on the final height of the compressed sample. Naturally, the mean structural parameter increases significantly with the recovery parameter, i.e. the effect of build-up due to particle interaction becomes more intensive, causing the material to regain its solid structure.

For a=0.1, structure build-up is so slow that the experiment stops when λ is slightly above its minimum value. Obviously, the effect of the break-down parameter b is opposite to that of a. Therefore, as shown in Figure 6, the rate of squeezing increases with b, i.e. the structure break-down becomes faster. The results for $\bar{\lambda}$ confirm that by increasing b the material bonds are forced to break-up faster with significant reduction of the mean structural parameter. When b=5, λ is reduced significantly down to 0.1 in a relatively short time and then increases steadily as structure is build-up.

Let us now consider the squeeze flow under constant velocity with V=-1, Re=1, Bn=1, a=1, b=1, and c=0.01. The required load for compressing the material is plotted in Figure 7. Initially the load is very high and decreases rapidly reaching a minimum after which a progressive increase occurs. Later, as the sample top surface expands, the load increases exponentially. At a certain critical time the simulation is stopped, due to excessive distortion of the finite elements (the sample becomes very thin). It should be noted that a smoothing of the load curve has been employed, in order to eliminate artificial spikes in the pressure (and hence in the calculation of the load) due to the discrete advancing of the nodal points on the solid surface.

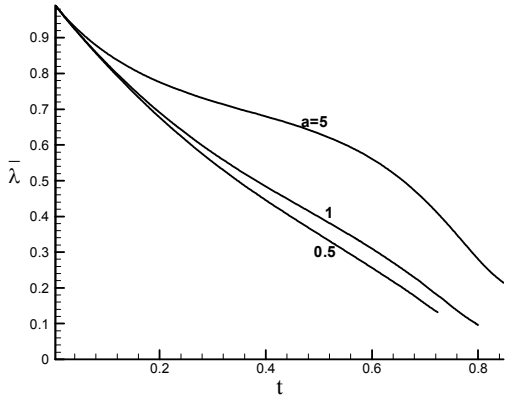

Figure 8: Effect of the recovery parameter on the evolution of the mean structural parameter during squeeze flow under constant velocity; V=-1, Re=1, Bn=1, b=1, and c=0.01.

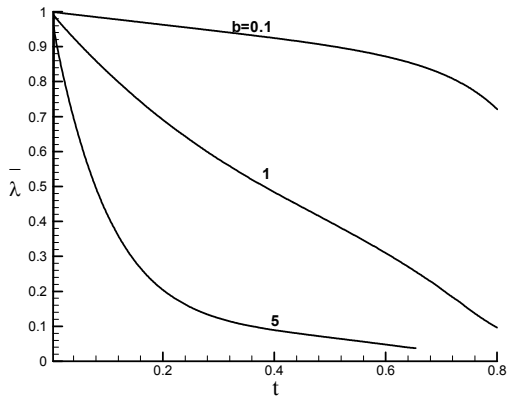

Figure 9: Effect of the breakdown parameter on the evolution of the mean structural parameter during squeeze flow under constant velocity; V=-1, Re=1, Bn=1, a=0.1, and c=0.01.

Simulations (not shown here for space reasons) show that the recovery and break-down parameters have relatively little effect on the resulting. Figures 8 and 9, respectively show the effects of a and b on the structure of the sample. Under constant velocity compression the structure essentially continues to break down in a manner very different from the compression under constant force. It is clear that break-down occurs faster for lower values of a and the entire phenomenon is irreversible (Figure 8). As expected, the structural parameter decreases significantly at higher values of b (Figure 9), a phenomenon which appears to be also irreversible.

When the sample is squeezed under constant velocity the average rate of strain is fixed by the velocity. The average strain everywhere within then sample increases with increasing compression. Therefore during compression the structure everywhere within the sample breaks down continuously. Therefore, except for extreme values of the recovery parameter, the structure is destroyed in relatively short time and the rate of buildup is not important. Possible unyielded regions within the sample disappear in a very short time. When however the sample is squeezed under constant force the situation is vey different. During compression as the sample is squeezed the compressed area increases. Therefore the imposed stress on the sample decreases. The flow and topography of the yielded and unyielded regions develop as a competition between the local stress , the rate of strain and both, the breakdown and recovery parameters. Both the flow field and the unyielded regions are more complex than the case of compression under constant velocity. These differences and the complexity of the resulting flow field show clearly that the only way to extract reliable data is by using computational rheology: the actual experiment must be simulated with high accuracy and by using reverse engineering extract the actual constants

Conclusions

The simulations show clearly that the results from the squeeze flow experiment can vary and they depend on whether the sample is squeezed under constant force or under constant velocity. These differences of course cannot be seen when the thixotropy is not accounted for. Material constants obtained with models that ignore thixotropy then will not characterize the rheology adequately. As the slurries are indeed thixotropic it is important to understand the different flows situations. By customizing the experiments it is possible to exploit these differences by isolating the effects of built up and breakdown.

References

[1] A.N. Alexandrou, Y. Pan, D. Apelian and G. Georgiou, "Semisolid material characterization using computational rheology," in Proceedings of the 7th International Conference on Semi-Solid Processing of Alloys and Composites, Y. Tsutsui, M. Kiuchi, K. Ichikawa (Eds.), Tsukuba, Japan (2002) 417-422.

[2] M. Modigell, J. Koke, Time-depended rheological properties of semisolid metal alloys, Mech. Time-Dependent Mater. 3 (1999) 15-30.

[3] L. Azzi, F. Ajersch, Analytical modelling of the rheological behavior of semisolid metals and composites, Metall. Mater. Trans. B 37 (2006) 1067-1074.

[4] V. Favier, H. Atkinson, Analysis of semi-solid response under rapid compression test using multi-scale modelling and experiments, Trans. Nonferrous Met. Soc. China 20 (2010) 1691-1695.

[5] J. Koke, M. Modigell, Flow behavior of semi-solid metal alloys, J. Non-Newtonian Fluid Mech. 112 (2003) 141-160.

[6] A.N. Alexandrou, G. Georgiou, On the early breakdown of semisolid suspensions, J. Non-Newtonian Fluid Mech. 142 (2007) 199-206.

[7] B.P. Gautham, P.C. Kapur, Rheological model for short duration response of semi-solid metals, Mat. Sci. Eng. A393 (2005) 223-228.

[8] R. Koeune, J.-P. Ponthot, An improved constitutive model for the numerical simulation of semi-solid thixoforming, J. Comp. Appl. Math. 234 (2010) 2287-2296.

[9] A. Potanin, 3D simulation of the flow of thixotropic fluids, in large-gap Couette and vane-cup geometries, J. Non-Newtonian Fluid Mech. 165 (2010) 299-312.

[10] H.A. Ardakani, E. Mitsoulis, S.G. Hatzikiriakos, Thixotropic flow of toothpaste through extrusion dies, J. Non-Newtonian Fluid Mech. 166 (2011) 1762-1271.

[11] D.N. Smyrnaios, J.A. Tsamopoulos, Squeeze flow of Bingham plastics, J. Non-Newtonian Fluid Mech. 100 (2001) 165-190.

[12] J. Engmann, C. Serrais, A.S. Burbidge, Squeeze flow theory and applications to rheometry: A review, J. Non-Newtonian Fluid Mech. 132 (2005) 1-27.

[13] P. Kumar, C.L. Martin, S. Brown, Constitutive modeling and characterization of the flow behavior of semi-solid metal alloy slurries. I. The flow response, Acta Met. Mater. 42(11) (1994) 3595-3602.

[14] G.C. Florides, A.N. Alexandrou, G. Georgiou, Flow development in compression of a finite amount of a Bingham plastic, J. Non-Newtonian Fluid Mech. 143 (2007) 38-47.

[15] G.R. Burgos, A.N. Alexandrou, V.M. Entov, Thixotropic behavior of semisolid slurries, J. Mater. Process Techn. 110 (2001) 164-176.

[16] T.C. Papanastasiou, Flows of materials with yield, J. Rheol. 31 (1987) 385-404.

[17] K.R.J. Ellwood, G.C. Georgiou, T.C. Papanastasiou, J.O. Wilkes, Laminar jets of Bingham-plastic liquids, J. Rheol. 34 (1990) 787-812.